Journal of Experimental Biology and Agricultural Sciences, April - 2022; Volume – 10(2) page 369 – 378

Journal of Experimental Biology and Agricultural Sciences

http://www.jebas.org

ISSN No. 2320 – 8694

Dynamics of land-use Change using Geospatial Techniques From 1986 to 2019: A Case Study of High Oum Er-Rbia Watershed (Middle Atlas Region)

Younes OULARBI[1,*], Jamila DAHMANI[1], Fouad MOUNIR[2]

[1]Department of Biology, Laboratory of Plant, Animal and Agro-Industry Productions, Faculty of Sciences, Ibn Tofail University, Kénitra, Morocco.
[2]National Forestry School of Engineers, 511 Salé, Morocco.

Received – January 22, 2022; Revision – March 17, 2022; Accepted – April 29, 2022
Available Online – April 30, 2022

DOI: http://dx.doi.org/10.18006/2022.10(2).369.378

KEYWORDS

Google Earth Engine (GEE)

Random Forest (RF)

Environmental changes

Spatio-temporal changes

Remote sensing

Landsat

Land use map

ABSTRACT

This work aims to expose the contribution of the use of the cloud google earth Engine (GEE) platform, in particular the capacity of optical monitoring by remote sensing to assess the impact of environmental changes on the evolution of natural resources in the Middle Atlas region. To achieve this goal, the dense time stacking of multi-temporal Landsat images and random forest algorithm based on the Google Earth Engine (GEE) platform was used. The spatial resolution of the images used is 30 meters for the TM 5 sensor (Thematic Mapper) and the OLI 8 sensor (Operational Land Imager). Further, the google earth engine platform is used primarily to download and prepare the images for the dates 1986, 2000, and 2019, then a supervised classification with the Random Forest (RF) algorithm to produce land use maps of selected dates with an overall accuracy exceeding 80%. This was followed by the production of maps and change matrices for the periods 1986-2000 and 2000-2019. The results obtained have shown a decline in grassland, forest land, and water body in parallel with an increase in the following classes: buildings, farmland, and arboriculture during the last 30 years. In addition, elevation was the most important characteristic variable for land-use classification in the study area. Obtained results provide theoretical support for adjusting and optimizing land use in the High Oum Er-Rbia watershed.

* Corresponding author

E-mail: younes.oularbi@uit.ac.ma (Younes OULARBI)

Peer review under responsibility of Journal of Experimental Biology and Agricultural Sciences.

Production and Hosting by Horizon Publisher India [HPI] (http://www.horizonpublisherindia.in/).

1 Introduction

The Middle Atlas is one of the three great mountain ranges which constitute the framework of the Moroccan geographical space, and these are (i) the Rif in the North, (ii) the Middle and High Atlas in the center, and (iii) the Anti-Atlas in the South (De Waele and Melis 2009). This chain is also characterized by its varied natural resources and its situation as a transit zone. In this mountainous region, the altitudes vary between 600 and 2400 m; and it contains the most beautiful cedar groves in Morocco and the Mediterranean basin. Over the past few decades, human population and activity have seriously threatened biodiversity, ecosystem services, and wildlife habitat. This World's ecological heritage is of major economic, social, cultural, and tourist interest, hence there is a strong need for its conservation and development.

Land use and land cover changes are one of the most important planner issues in recent years because most of these changes are not expected and appear as environmental degradation, water scarcity, and worsening food security (Rasool et al. 2021). In addition, these changes describe the impact of anthropogenic disturbance on the surface of the Earth and play an important role in the studies of regional and global environmental changes (Ran et al. 2019). Land use is the result of the interaction between land's natural vocation and cultural backgrounds (Tsai et al. 2019).

Land cover change is directly linked with land use and gives rise to the degradation of multiple ecosystems (Schürmann et al. 2020). Physical and socio-economic factors are the most important drivers of land-use change they are very important for the modeling of land-use change. These changes in land use and land cover can be described as a factor of change inducing environmental change since they are the basis of either the reduction or the amplification of greenhouse gas emissions and therefore (MEA 2005).

To prevent and control the effects of land cover and land use changes we need a relevant knowledge of the stat of land cover and land use and the changes associated with these (Anderson 1976). Currently, thanks to the development of earth observation science that makes available the remote sensing data of different dates and locations of the world, detection, and monitoring of land-use change effects can be done at the local and global level (Rogan and Chen 2004).

The combined exploitation of GIS and remote sensing techniques allows the mapping and land use perdition as well as the identification of the different spatial and temporal transitions of these changes (Lillesand et al. 2015), the research using high-resolution images from different dates and GIS techniques under a geospatial modeling environment can provide relevant information for planning environmental and economic development programs to combat the negative effects of environmental changes (MEA 2005).

The Google Earth Engine (GEE) provides a JavaScript and Python coding environment to facilitate multi-source satellite data processing for the user can without downloading and pre-processing the data (Tamiminia et al. 2020).

This study applied dense time stacking of Landsat images to monitor land cover changes in the High Oum Er-Rbia watershed. This study aimed to obtain the land cover and land cover changes information of the High Oum Er-Rbia watershed from 1986 to 2019 based on the GEE platform. The results are expected to provide theoretical support for adjusting and optimizing land use in the High Oum Er-Rbia watershed.

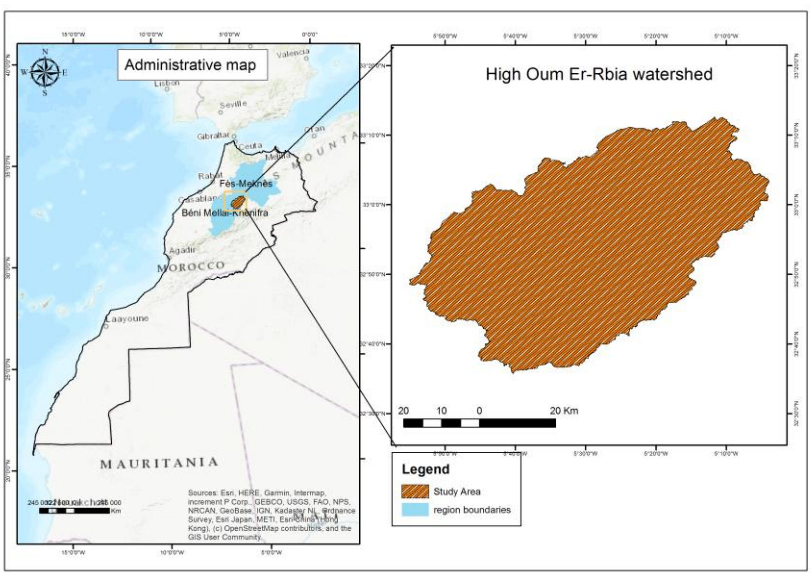

Figure 1 Location of the study area.

2 Materials and Methods

2.1 Study area

The study area is located in the southwest of the central Middle Atlas Mountain in the Beni mellal-Khenifra region, between 32°35’N to 33°12’ N latitude and 5°03’W to 5°55’W longitude. It covers more than 3600 km² (El Jazouli et al. 2019). The geographical landscape presents attitudes that can go from 700 m up to 2400m from the high mountains. According to the geological maps the geological formations of the studied, range from Paleozoic to Quaternary, consisting of sub tabular limestone rocks and Liassic dolomitic limestones. The study area is characterized by a Mediterranean climate known for warm/hot and dry summers and mild/cool and wet winters. The annual average precipitation is between 400 and 700 mm, and the minimum and maximum temperature's usual values are respectively 5 and 50°C. The forest vegetation consists mainly of holm oaks and cedars which are mainly located in the upper and middle part of the watershed. The average population density of the study area is 42.32 ha/km^2 according to the 2014 General Population and Housing Census. The Oum Er Rbia River and its tributaries of Srou and Chbouka, crossing the Atlas Mountain chain, drain the studied watershed.

2.2 Data preparing

Google Earth Engine is a platform for worldwide geospatial analysis on diverse matters of which we can cite deforestation, climate change monitoring, environmental issues, and water management (Gorelick et al. 2017). The GEE provides Landsat datasets by the United States Geological Survey (USGS, https://www.usgs.gov/) and all acquired Landsat images, are pre-processed, mosaicked, and processed through the JavaScript application programming interface (API) (Bootsma 2021).

In this work, all processing of Landsat TM and OLI data was conducted on the GEE platform (https://earthengine.google.com) and in a free GIS environment, the available Landsat TM and OLI Collection 1 Tier 1 top of atmosphere (TOA) reflectance products in the High Oum Er-Rbia watershed were analyzed.

The image processing includes the following steps (i) filter and selects all satellites images (TOA reflectance product) of the period (May–September), (ii) The clouds were removed from the Landsat images of the study area, (iii) then a single image was generate from the image collection by using a reducer function (Pu et al. 2020), (iv) The normalized difference vegetation index (NDVI), the normalized difference-built index (NDBI), and the Modified Normalized Difference Water Index (MNDWI) (MNDWI) were calculated for each image and (v) The slope and aspect from DEM data were added to perform the classification. Therefore, the best image is obtained by a combination of images, cloud-free, combining NDVI, NDBI, MNDWI, slope, and aspect.

2.3 Training and Validation Sample Selection

The classification system was determined based on current land use in the High Oum Er-Rbia watershed. In compliance with previous research in the Hight Oum Ee Rbia watershed (El-Bouqdaoui 2007), we adopted seven major land-use types: forest, arboriculture, rangeland, farmland, and buildings, water bodies, and unused land (other lands).

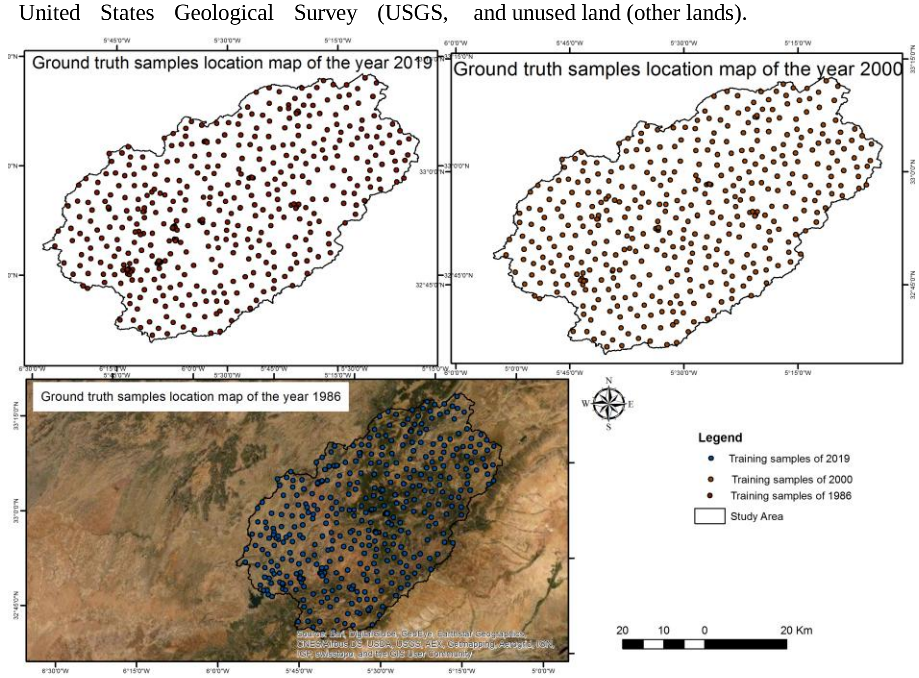

Figure 2 Plot distribution in the High Oum Er-Rbia watershed

Training samples used to create the classification model were collected through (i) visual interpretation of the very high-resolution image on different year's satellites images and (ii) field observations from the area study. In total, more than 1300 plots (440 plots for each year) were collected with more than 40 samples for each land-use type, 70% of which were randomly selected as participants in classification as training samples, and 30% used to verify the classification results as validation samples (Figure 2).

2.4 Method

The methodology is based on using Landsat images on the GEE platform. Whose images were pre-processed by date filtering, cloud masking, mosaicking, and clipping to obtain a Landsat TOA composite image and to calculate the characteristic parameters to implement the later classification. Then the training and validation sample datasets already uploaded to the GEE were implemented in the classification. In this study, the random forest (RF) machine learning algorithm was used. The results were validated using a confusion matrix. Finally, the land use transfer matrix was used to analyze the change in each land-use type for each year type in the High Oum Er-Rbia watershed (figure 3).

In the current study, the random forest (RF) algorithm was selected because it can deal with complex data of large dimensions and can usually provide higher accuracy than other traditional algorithms, such as maximum likelihood and single decision tree (Belgiu and Dragut 2016; Na et al. 2010). The classifier can be presented as an ensemble learning method that creates random features and uses them to generate multiple decision trees and classifies a dataset by using the prediction modes of all decision trees (Tamiminia et al. 2020).

RF has even proven to give good results when used in various applications such as land cover classification on multi-temporal and multi-frequency SAR data (Waske and Braun 2009). The relative importance of each target variable class could be measured with the RF classifier (Rodriguez-Galiano et al. 2012).

In this study GEE platform and RF algorithm was applied based on the field's simples to obtain the Land use classification maps for each separate year, the number of trees was set to 500 and the number of classes is fixed to 7 classes. To evaluate the accuracy of remote sensing image classification, the confusion matrix was produced. The matrix provides the correspondence between the land-use classification results and verification data. In this work, the verification of classification accuracy is reflected by overall accuracy, kappa coefficient, producer's accuracy, and user's accuracy.

3 Results and discussions

In this work, a total of 176 satellites images were used (Table 1). All images are free from cloud cover and are part of the Landsat 5 TM and Landsat 8 OLI collection. Favorite

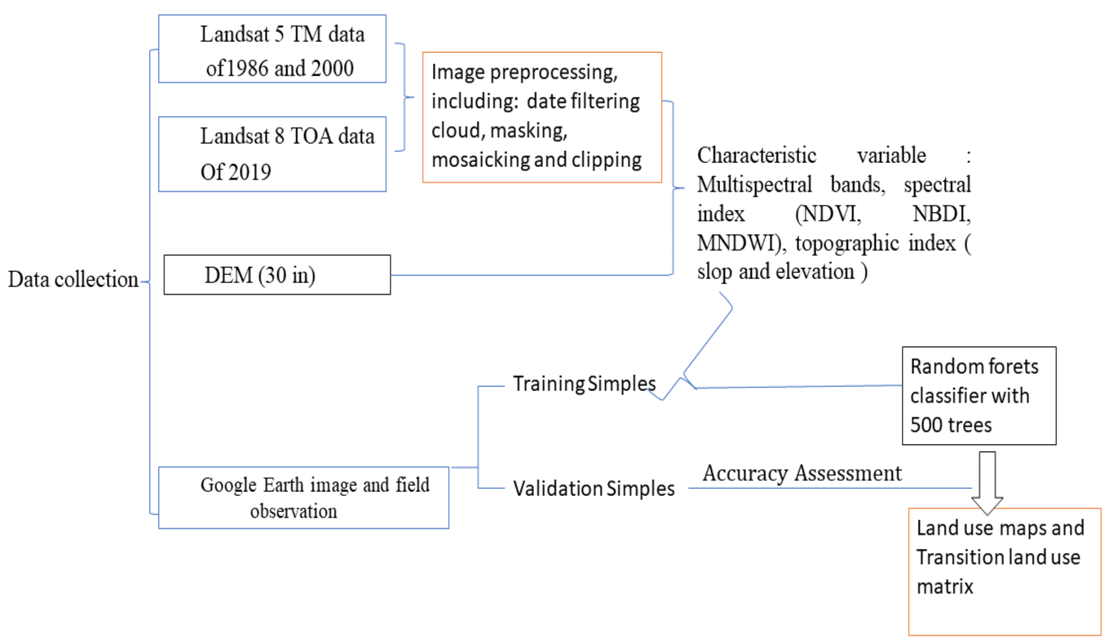

Figure 3 Methodology used for the characterization of spatial and temporal changes in land cover in the study area

Table 1 Characteristics of taken Images

Satellite	Years	Paths	Rows	Number of images	Cloud cover
Landsat 5 TM	1985-1987	200-199	37-38	27	0%
Landsat 5 TM	1999-2001	200-200	37-38	67	0%
Landsat 8 OLI	2018-2020	200-201	37-38	82	0%

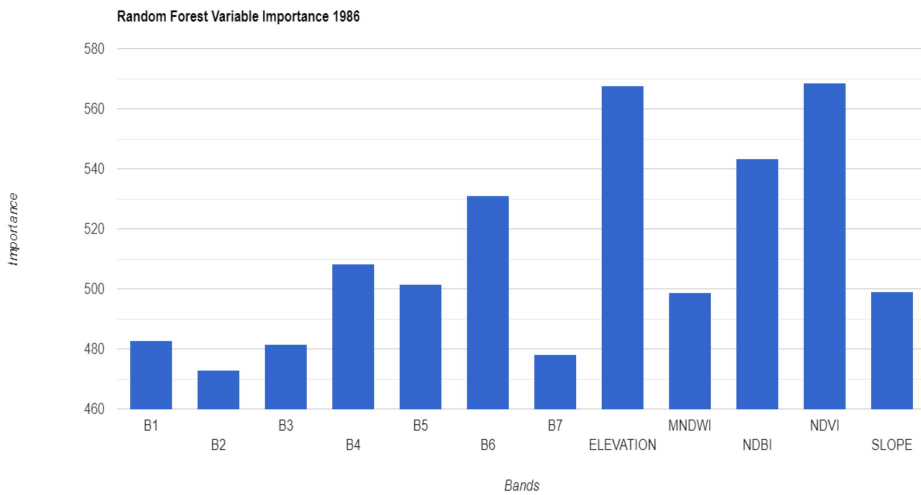

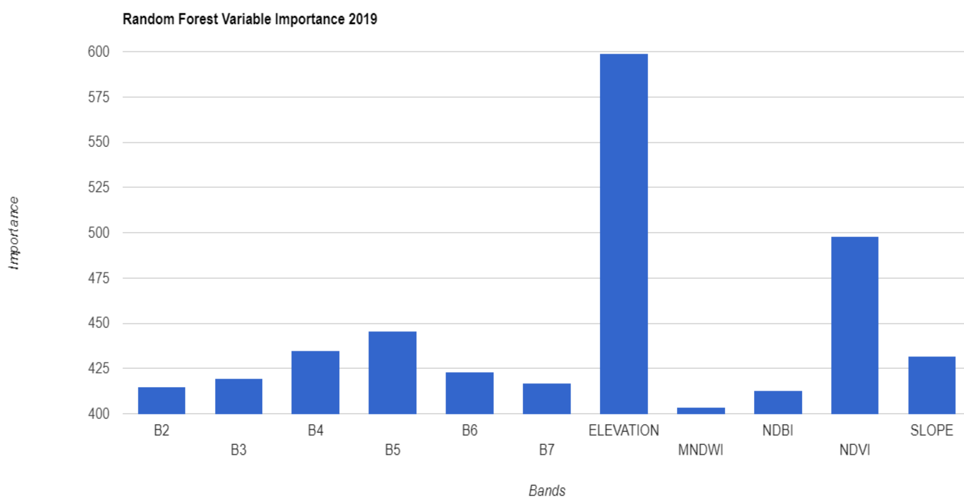

Figure 4 Importance distribution of characteristic variables in Land use classification

3.1 Variable Importance Analysis and Accuracy Assessment of Land-use classification

The RF model can analyze the importance of characteristic variables, which improves classification accuracy. The importance of characteristic parameters analyzed on the GEE platform can indicate the greater impact and contribution of the variable to the classification results. Results of the current study showed that elevation and the NDVI were the highest importance score among all the characteristic variables (Figure 4) and the slope, MNDWI, and NDBI were as followed. These results are in agreement with the findings of Hoshikawa and Umezaki (2014) those who found that terrain has a significant impact on land use classification.

The accuracy of the classification result is an important prerequisite for analyzing land-use changes. The classification results of the study showed that the overall accuracy was 85%, 87%, and 86% for 1986, 2000, and 2019, respectively, and the kappa coefficient was 79%, 82%, and 90 % for 1986, 2000, and

Table 2 Confusion matrix of the classification shown (unit: %) .

Land use type	1986		2000		2019	
	User's Accuracy	Producer's Accuracy	User's Accuracy	Producer's Accuracy	User's Accuracy	Producer's Accuracy
Forest	0.92	0.96	0.91	0.93	0.92	0.95
Arboriculture	1	0.65	1	0.42	0.92	0.88
Rangeland	0.8	0.72	0.84	0.83	0.82	0.77
Farmdland	0.76	0.87	0.82	0.88	0.88	0.9
Buildings	1	1	1	0.5	0.9	0.9
Water	0.69	1	1	0.86	1	0.8
Other	1	0.41	0.8	0.67	1	1
Overall accuracy	0.85		0.87		0.86	
Kappa Coefficient	0.79		0.82		0.9	

2019, respectively (Table 2). The overall accuracy of the classification reached the acceptable threshold, indicating that the classification accuracy could meet the requirements of the land-use classification. The confusion matrix showed detailed classification accuracy for each land-use type (Table 2).

3.2 Spatiotemporal Characteristics of land use Changes

The GEE platform classification results are shown after applying the model (figure 5), and the Land-use maps of the study area in 1986, 2000, and 2019 are shown in (figure 6). Forest land was the main land use type, occupying more than 45% of the total land area while the farmland land was the second main land use type with an area ratio of approximately 40% and the Rangeland covers approximately 15 % of the total land area. The construction land, arboriculture, water body areas were the smallest, less than 5% of each one. These results are confirmed by the study of EL-Bouqdaoui (2007).

From 1986 to 2019, the area of forest land, arboriculture land, and construction expanded, especially the percentage of arboriculture land area, which increased from 0.71% to 4%. However, during the study period, the Rangeland and wetland gradually decreased (Figure 6).

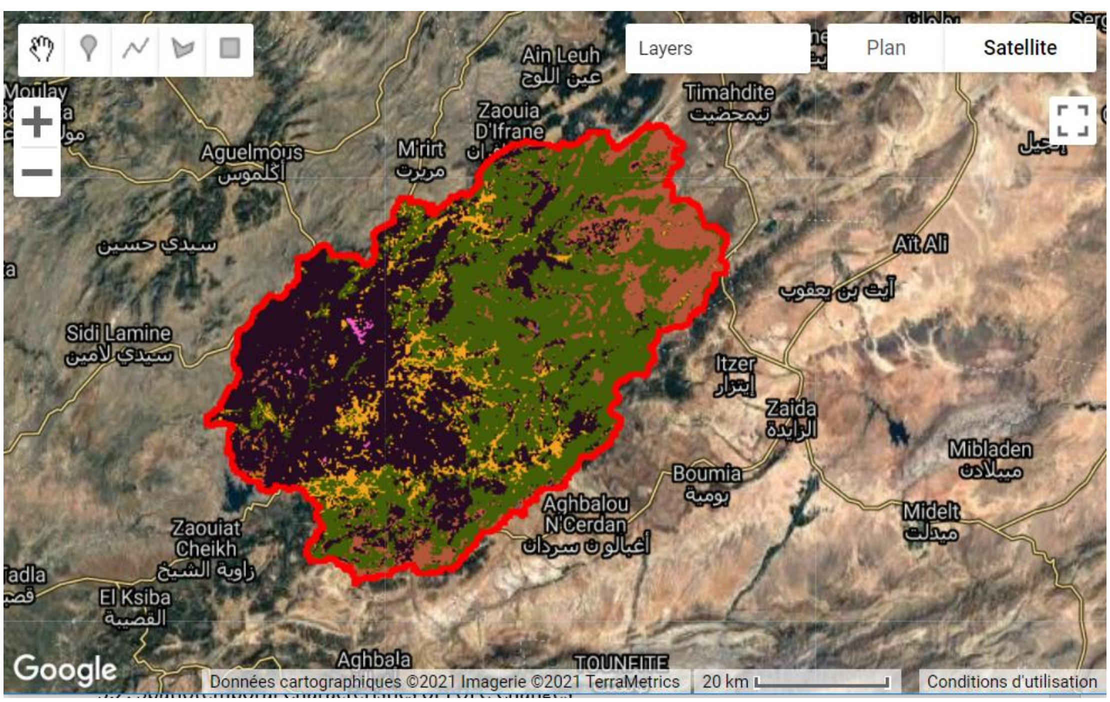

Figure 5 GEE classification result on 2019

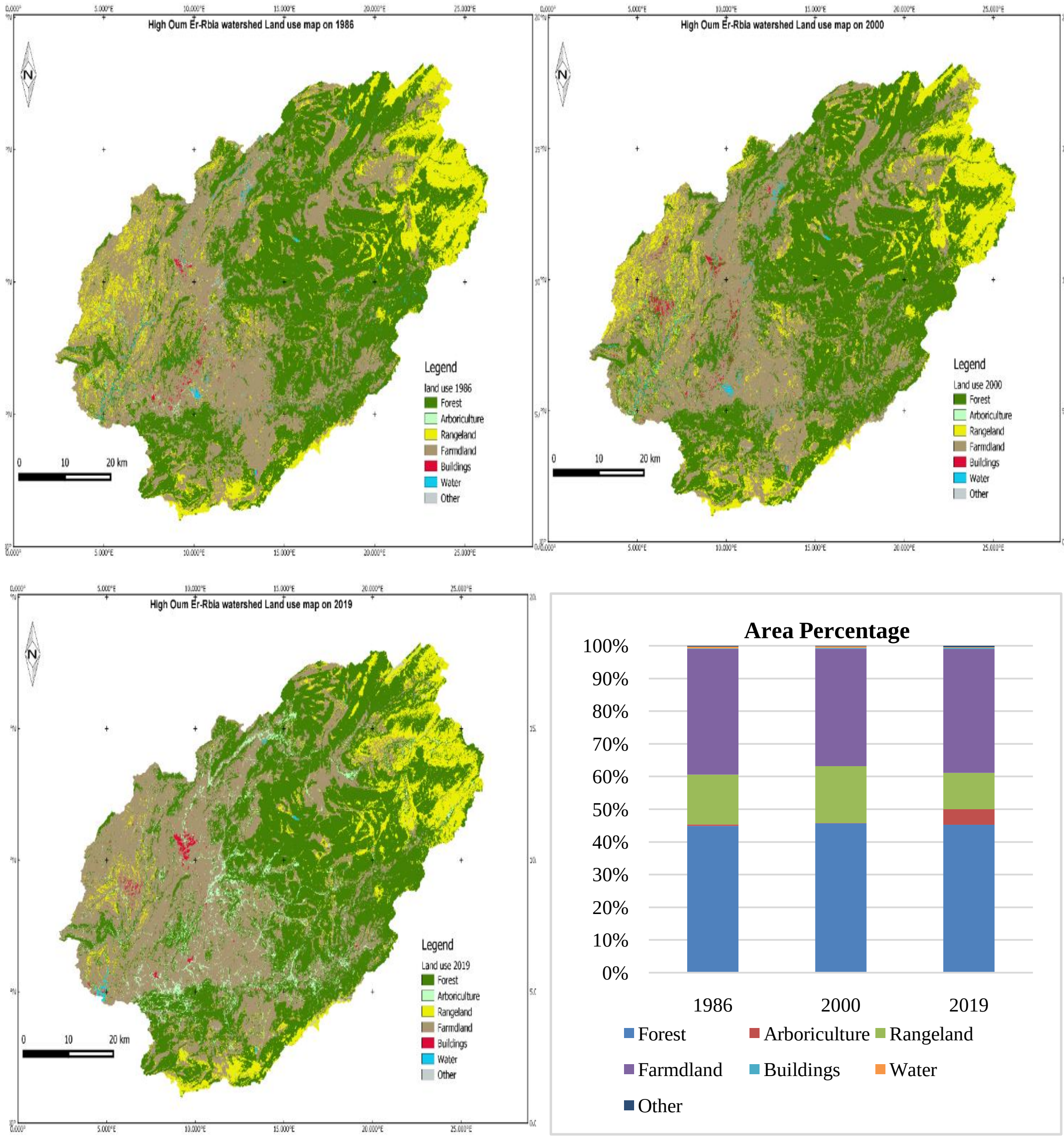

Figure 6 Hight Oum Er- Rbia watershed land use maps on 1986, 2000, and 2019 and area percentage of land use type in the study area

3.3 Land use transformation from 1986 to 2019

To observe the changes in various land-use types, we used the spatial analysis method to study the land-use changes transition matrix from 1986 to 2019 and mapped them. From 1986 to 2000, in general, forest land, Rangeland, and buildings were expanded, while the area covered by Arboriculture, farmland, and water body decreased (Tables 3 and 4).

Among the study areas, 12234 hectares of farmland and 4282 hectares of rangeland were transformed into forest land respectively. The expansion of construction land came essentially from farmland, while the forest land was mainly converted into farmland and rangeland (Table 3). In addition, approximately 712 hectares of water body was converted to Forest land and farmland.

Similarly, from 2000 to 2019, the areas of forest land and rangeland continued to decrease, while arboriculture, farmland, and water bodies expanded. The arboriculture was mainly increased from forest land (6250 hectares), farmland (5742 hectares), and rangeland (364 hectares) (Table 4).

Table 3 Matrix of land use change between 1986 and 2000 (unit: hectares)

		2000							Total 1986
		Forest	Arboriculture	Rangeland	Farmdland	Buildings	Water	Other	
1986	Forest	127190	46	4300	9488	5	15	24	141067
	Arboriculture	886	79	80	1154	8	2	1	2210
	Rangeland	4282	1	26100	11594	29	20	62	42087
	Farmdland	12234	28	15182	94607	978	141	123	123292
	Buildings	44	0	10	469	158	0	0	681
	Water	494	3	33	185	7	313	47	1083
	Other	64	1	56	169	0	7	87	385
Total 2000		145194	157	45760	117667	1185	498	344	310805

Table 4 Matrix of land use change between 2000 and 2019 (unit: hectares)

		2019							Total 2000
		Forest	Arboriculture	Rangeland	Farmdland	Buildings	Water	Other	
2000	Forest	125567	6250	2037	10902	165	163	109	145194
	Arboriculture	3	136	0	16	0		1	157
	Rangeland	5522	364	22379	17383	41	50	14	45760
	Farmdland	12383	5742	4623	93793	642	397	88	117667
	Buildings	2	12	1	831	330	6	3	1185
	Water	46	28	73	254	1	1	94	498
	Other	4	6	199	59	2	73	1	344
Total 2019		143528	12538	29312	123239	1182	689	310	310805

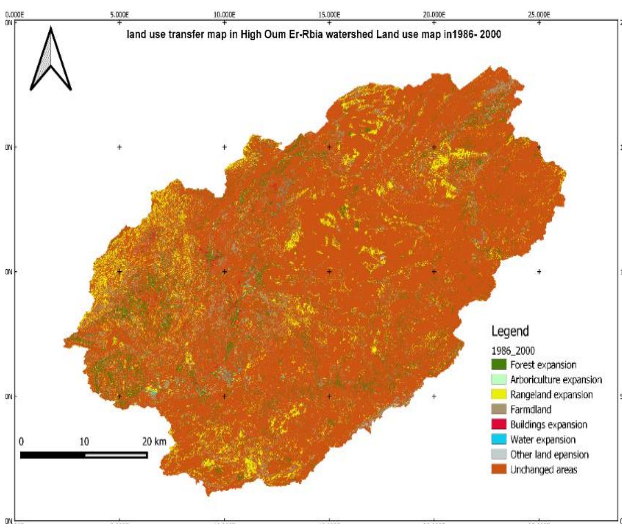

Figure 7 land use transfer map in 1986-2000

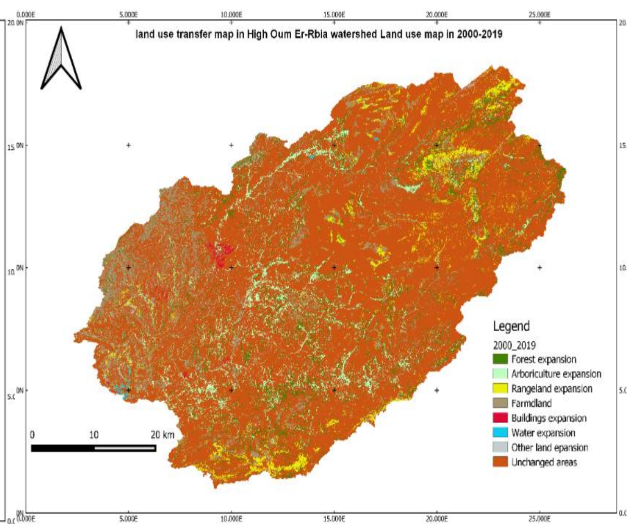

Figure 8 Land use transfer map in 2000-2019

Comparing the spatial-temporal changes in land use between 2000–2009 and 2009–2018 (figures 7 and 8), it was found that the arboriculture area decreased first and then increased, but the forest land area followed the opposite trend. In general, between 1986 and 2019, the rangeland and water were continuously degraded, and the areas of forest land, construction land, and arboriculture gradually increased.

3.4 Analysis of land use Classification Variable Importance and Result Verification

This study extracted 12 characteristic variables from satellite imagery and used the RF classifier on the GEE platform to classify land use in the High Oum Er-Rbia watershed. The RF method allows multiple data sources to be used in the modeling process and classifies land-use heterogeneity properly (Breiman 2001). The variable importance analysis shows that elevation is the main important factor that contributes to the land use classification (Figure 4) in addition to the MNDWI and NDVI which are used to extract vegetation and water present in the study area.

The overall accuracy and kappa coefficient for this study is higher than 80% which is a good result (Gashaw et al. 2018), Accurate training samples and validation samples are the basis of the classification accuracy. Arboriculture and forestland land-use type show the highest user accuracy and producer's accuracy of land use classification results from 1986 to 2019 (Table 2).

3.5 Temporal-Spatial Variation of land use Changes

Land-use changes are influenced by the interaction between humans and the environment at different spatial and temporal scales. Monitoring Land use changes can help us understand the causes of their dynamic changes, and it supports land management and decision-making (Ren et al. 2017; Ren et al. 2018). The land-use classification results indicated that forest land was the main land-use type in the high Oum Er- Rbia watershed, followed by farmland land and grassland.

Comparing land-use changes in the Oum Er- Rbia watershed in the periods of 1986−2000 and 2000−2019. The change trajectories of the main land-use types in the periods of 1986−2000 and 2000−2019 were the same. The forest land has continued to decline, but the arboriculture and farmland land show the opposite trend. The buildings area expanded but the water body broadly decreased from 1986.

The difference can probably be attributed to the implementation of the Project of Green Morocco plan. The expansion of construction land was faster after 2000. Moreover, the wetland area decreased from 1986 to 2019, which was mainly due to the drought: a decrease in annual mean precipitation and dry lakes even with the establishment of the Ahmed El Hansalidam commissioned in 2002 there was still a decrease.

Conclusions

The study used the dense time stacking of multi-temporal Landsat images and the RF machine learning algorithm to map the land use in the high Oum Er- Rbia watershed. Our results demonstrated that from 1986 to 2019, the study area was dominated by forestland, followed by farmland land and grassland. Grasslands and wetlands gradually degraded from 2000 to 2018, while farmland land, arboriculture, construction land, and unused land expanded. Grassland was mainly converted to Farmland and arboriculture land. In addition, the importance analysis of all variables using the RF model found that elevation and NDVI were the most important characteristic variable for land-use classification in the high Oum Er- Rbia watershed.

References

Anderson, J. R. (1976). *A land use and land cover classification system for use with remote sensor data* (Vol. 964). US Government Printing Office.

Belgiu, M., & Dragut, L. (2016). Random forest in remote sensing: A review of applications and future directions. *ISPRS Journal of Photogrammetry and Remote Sensing*, *114*, 24–31.

Bootsma, E. J. (2021). Mapping time-series evapotranspiration for agricultural applications (Unpublished Dissertation).

Breiman, L. (2001). Random forests. *Machine Learning*, *45* (1), 5–32.

De Waele, J., & Melis, M. T. (2009). Geomorphology and geomorphological heritage of the Ifrane–Azrou region (Middle Atlas, Morocco). *Environmentalgeology*, *58*(3), 587-599.

El-Bouqdaoui, K. (2007). Approche méthodologique de l'évaluation du risque potentiel d'érosion des sols du bassin versant du Srou (Moyen Atlas, Maroc) à l' aide de la télédétection et du SIG.

El Jazouli, A., Barakat, A., Khellouk, R., Rais, J., & El Baghdadi, M. (2019). Remote sensing and GIS techniques for prediction of land use land cover change effects on soil erosion in the high basin of the Oum Er Rbia River (Morocco). *Remote Sensing Applications: Society and Environment*, *13*, 361-374.

Gashaw, T., Tulu, T., Argaw, M., Worqlul, A.W., Tolessa, T., & Kindu, M. (2018). Estimating the impacts of land use/land cover changes on ecosystem service values: The case of the Andassa watershed in the Upper Blue Nile basin of Ethiopia. *Ecosystem Services*, *31*, 219–228.

Gorelick, N., Hancher, M., Dixon, M., Ilyushchenko, S., Thau, D., & Moore, R. (2017) Google earth engine: planetary-scale geospatial analysis for everyone. *Remote Sensing Environment*, *202*(1), 18–27.

Hoshikawa, K., & Umezaki, M. (2014). Effects of terrain-induced shade removal using global DEM data sets on land-cover classification. *International Journal of Remote Sensing*, *35*(4), 1331-1355.

Lillesand, T., Kiefer, R. W., & Chipman, J. (2015). *Remote sensing and image interpretation*. John Wiley & Sons.

Millennium Ecosystem Assessment. (2005). Ecosystems and Human Well-being. Opportunities and challenges for Business and Industry. . Retrieved from https://www.millenniumassessment.org/documents/document.353.aspx.pdf.

Na, X.D., Zhang, S.Q., Li, X.F., Yu, H.A., & Liu, C.Y. (2010).Improved land cover mapping using random forests combined with landsat thematic mapper imagery and ancillary geographic data. *Photogrammetric Engineering & Remote Sensing*, *76*, 833–840.

Ran, Q., Hao, Y., Xia, A., Liu, W., et al. (2019). Quantitative assessment of the impact of physical and anthropogenic factors on vegetation spatial-temporal variation in Northern Tibet. *Remote Sensing*, *11*(10), 1183.

Rasool, R., Fayaz, A., ul Shafiq, M., Singh, H., & Ahmed, P. (2021). Land use land cover change in Kashmir Himalaya: Linking remote sensing with an indicator based DPSIR approach. *Ecological Indicators*, *125*, 107447.

Ren, M., Zeng, W., Yang, B., & Urtasun, R. (2018). Learning to reweight examples for robust deep learning. *In International conference on machine learning* (pp. 4334-4343). PMLR. Retrieved from http://proceedings.mlr.press/v80/ren18a/ren18a.pdf

Ren, Y., Lü, Y., Fu, B., & Zhang, K. (2017). Biodiversity and ecosystem functional enhancement by forest restoration: A meta-analysis in China. *Land Degradation & Development, 28(7),* 2062-2073.

Rodriguez-Galiano, V. F., Ghimire, B., Rogan, J., Chica-Olmo, M., & Rigol-Sanchez, J. P. (2012). An assessment of the effectiveness of a random forest classifier for land-cover classification. *ISPRS journal of photogrammetry and remote sensing*, *67*, 93-104.

Rogan, J., & Chen, D. (2004). Remote sensing technology for mapping and monitoring land-cover and land-use change. *Progress in planning*, *61*(4), 301-325.

Pu, D. C., Sun, J. Y., Ding, Q., Zheng, Q., Li, T. T., & Niu, X. F. (2020). Mapping urban areas using dense time series of landsat images and google earth engine. *The International Archives of Photogrammetry, Remote Sensing and Spatial Information Sciences*, *42*, 403-409.

Schürmann, A., Kleemann, J., Fürst, C., & Teucher, M. (2020). Assessing the relationship between land tenure issues and land cover changes around the Arabuko Sokoke Forest in Kenya. *Land Use Policy*, *95*, 104625.

Tamiminia, H., Salehi, B., Mahdianpari, M., Quackenbush, L., Adeli, S., & Brisco, B. (2020). Google Earth Engine for geo-big data applications: A meta-analysis and systematic review. *ISPRS Journal of Photogrammetry and Remote Sensing*, *164*, 152-170.

Tsai, Y. H., Stow, D., An, L., Chen, H. L., Lewison, R., & Shi, L. (2019). Monitoring land-cover and land-use dynamics in Fanjingshan National Nature Reserve. *Applied Geography*, *111*, 102077.

Waske, B., & Braun, M. (2009). Classifier ensembles for land cover mapping using multitemporal SAR imagery. *ISPRS journal of photogrammetry and remote sensing*, *64*(5),450-457.